Supporting information for “Condensation of excitons in a trap”

A.A. High,[1] J.R. Leonard,[1] M. Remeika,[1] L.V. Butov,[1] M. Hanson,[2] and A.C. Gossard[2]

[1]*Department of Physics, University of California at San Diego, La Jolla, CA 92093-0319, USA*

[2]*Materials Department, University of California at Santa Barbara, Santa Barbara, CA 93106-5050, USA*

(Dated: April 18, 2012)

Structure

The CQW structure is grown by MBE. An n^+-GaAs layer with $n_{Si} = 10^{18}$ cm^{-3} serves as a homogeneous bottom electrode. The top electrodes are fabricated via e-beam lithography by depositing a semitransparent layer of Ti (2 nm) and Pt (8 nm). The device includes a $3.5 \times 30\mu$m diamond electrode, a 600 nm wide 'wire' electrode around the diamond, and 'outer plane' electrode. Two 8 nm GaAs QWs separated by a 4 nm $Al_{0.33}Ga_{0.67}As$ barrier are positioned 100 nm above the n^+-GaAs layer within an undoped 1 μm thick $Al_{0.33}Ga_{0.67}As$ layer. Positioning the CQW closer to the homogeneous electrode suppresses the in-plane electric field [1], which otherwise can lead to exciton dissociation.

Experimental setup. Shift-interferometry measurements.

We use a Mach-Zehnder (MZ) interferometer to probe coherence of indirect excitons (Fig. 2a in the main text). The emission beam is made parallel by an objective inside the optical dilution refrigerator and lenses. In the shift-interferometry measurements, the path lengths of arm 1 and arm 2 are set equal. The interfering emission images produced by arm 1 and 2 of the MZ interferometer are shifted relative to each other along x to measure the interference between the emission of excitons, which are laterally separated by δx. The shift δx is determined from the images produced by arm 1 and arm 2 (Fig. 2b,c in the main text). It is controlled by the interferometer mirrors. The emission is filtered by an interference filter of linewidth $\pm 5,$nm adjusted to the emission wavelength of indirect excitons $\lambda = 800\,$nm, see Fig. 1a. The signal is focused to produce an image of emission of indirect excitons. The image is recorded by a liquid-nitrogen cooled CCD. We measure emission intensity I_1 for arm 1 open, I_2 for arm 2 open, and I_{12} for both arms open, and then calculate

$$I_{\text{interf}} = (I_{12} - I_1 - I_2)/(2\sqrt{I_1 I_2}\,)\,. \tag{1}$$

In general, for two partially coherent sources located at $\mathbf{r}_1$ and $\mathbf{r}_2$, one has the relation [2],

$$I_{\text{interf}} = \cos\delta\theta(\mathbf{r}_1, \mathbf{r}_2)\,\zeta(\mathbf{r}_1, \mathbf{r}_2)\,, \tag{2}$$

where $\delta\theta(\mathbf{r}_1, \mathbf{r}_2)$ is the phase difference of the two sources and $\zeta(\mathbf{r}_1, \mathbf{r}_2)$ is their degree of coherence. In our experimental geometry, there is a small tilt angle α between the image planes of the two arms. As a result, the phase difference

$$\delta\theta(\mathbf{r}_1, \mathbf{r}_2) = q_t y + \phi(\mathbf{r}_1, \mathbf{r}_2) \tag{3}$$

has a component linear in y — the coordinate in the direction perpendicular to the tilt axis — which produces periodic oscillation of I_{interf}. The period of the interference fringes is set by $q_t = 2\pi\alpha/\lambda$. The coherence function $\zeta(\mathbf{r}_1, \mathbf{r}_2)$ for $\mathbf{r}_1 - \mathbf{r}_2 = \delta\mathbf{x}$ is given by the amplitude of these interference fringes.

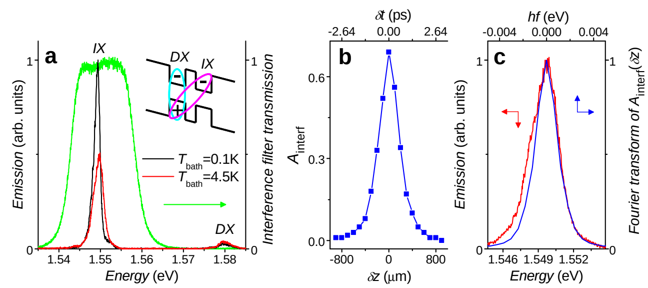

FIG. 1: (**a**) Emission spectra in the center of the trap for $T_{bath} = 0.1$ K (black line) and 4.5 K (red line) measured by spectrometer. Emission of direct excitons (DX) and indirect excitons (IX) is indicated. Green line presents the transmission curve of the interference filter used in the shift-interferometry, Fourier-spectroscopy, and imaging experiments. Inset: band diagram of the CQW with direct and indirect excitons. (**b**) Fourier-spectroscopy measurements: Amplitude of interference fringes A_{interf} vs. the difference in the path lengths of arm 1 and arm 2 of the MZ interferometer δz and corresponding time delay δt for indirect excitons in the center of the trap at $T_{bath} = 4.5$ K. (**c**) Calculated spectrum based on Fourier transform of $A_{\text{interf}}(\delta t)$ in (**b**) (blue line) and spectrum of indirect excitons measured by spectrometer in the center of the trap at $T_{bath} = 4.5$ K (red line). $P_{ex} = 1.9\,\mu$W.

Emission spectra. Fourier spectroscopy measurements.

Figure 1a presents the spectra at low and high temperature measured by spectrometer. In all interference and imaging experiments in the paper, only the emission of indirect excitons (IX) is measured. This is achieved by using an interference filter. The transmission curve of the interference filter is presented in Fig. 1a. This curve shows that the contribution of the weak emission of direct excitons (DX) or any other emission (such as

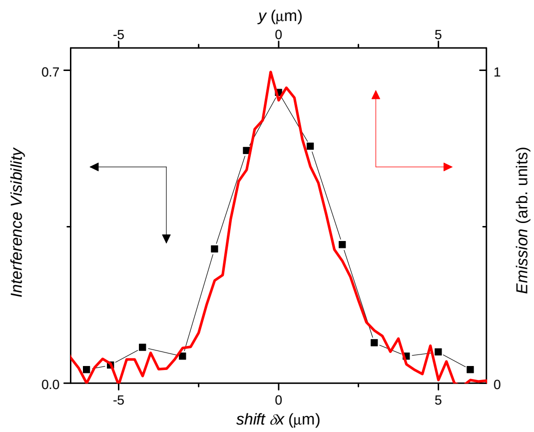

FIG. 2: Interference visibility vs. shift δx for excitons in trap at $T_{bath} = 8$ K (black squares) and y-axis cross section of exciton emission in a segment of the thin wire on the left from the diamond, see Fig. 1b in the main text (red line). The width of the wire, $0.6\,\mu$m, is significantly smaller than the spatial resolution and, therefore, the wire can be considered as a source of vanishing width.

low-energy bulk emission) has been cut off by the interference filter. Therefore, any change of the amplitude of the interference fringes $A_{interf}(\delta x)$ and, in turn, the coherence length measured in our experiments is due to a change of coherence of indirect excitons.

We also measured amplitude of interference fringes $A_{\rm interf}$ vs. the difference in the path lengths of arm 1 and arm 2 of the MZ interferometer δz and corresponding time delay δt for indirect excitons in the center of the trap (Fig. 1b). The spectrum obtained by this Fourier-spectroscopy measurement is in a good agreement with the spectrum measured by spectrometer (Fig. 1c).

Measurement of the point-spread function.

The point-spread function (PSF) of the optical setup is measured by exciting a segment of the thin wire on the left from the diamond (see Fig. 1b in the main text) and measuring the spatial profile of exciton emission across the wire (Fig. 2). The width of this wire is $0.6\,\mu$m, significantly smaller than the PSF width for our optical setup. Therefore, the wire can be considered as a source of vanishing width so the spatial profile of exciton emission across the wire is given by the PSF. This independent measure of the PSF is in good agreement with the $A_{interf}(\delta x)$ function at high temperatures $T \gtrsim 4$ K (Fig. 5 in the main text) that is given by the PSF width.

Interference images.

In this section, we present examples of interference images and their cross-sections providing technical details to the data presented in the main text of the paper.

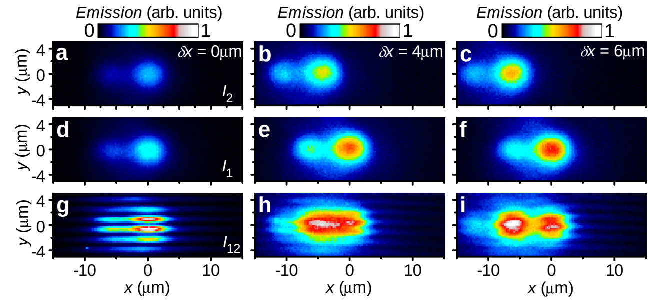

FIG. 3: Emission images I_2 for arm 2 open (a-c), emission images I_1 for arm 1 open (d-f), and interference images I_{12} for both arms open (g-i) for shift $\delta x = 0$ (a,d,g), $4\,\mu m$ (b,e,h), and $6\,\mu m$ (c,f,i). $T_{bath} = 0.1$ K, $P_{ex} = 1.9\,\mu$W.

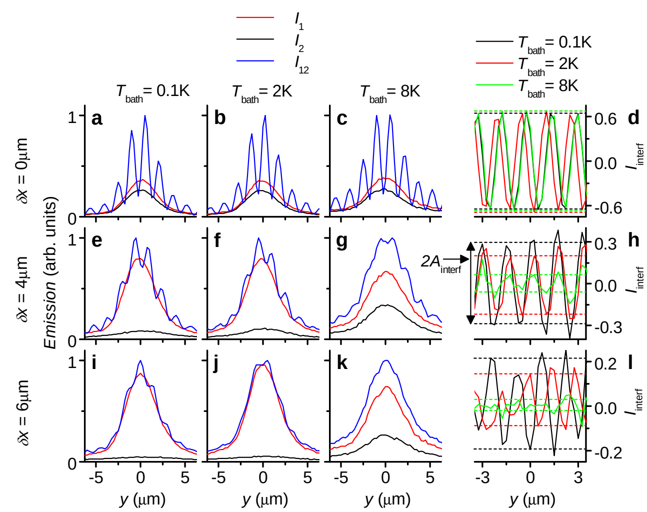

FIG. 4: (a-c, e-g, i-k) Spatial profiles along y at $x = 0$ of I_1 (red), I_2 (black), and I_{12} (blue) at shift $\delta x = 0$ (a-c), $4\,\mu m$ (e-g), and $6\,\mu m$ (i-k). $T_{bath} = 0.1$ K (a,e,i), 2 K (b,f,j), and 8 K (c,g,k). (d,h,l) Spatial profiles along y at $x = 0$ of $I_{\rm interf}$ at $T_{bath} = 0.1$ K (black), 2 K (red), and 8 K (green) for $\delta x = 0$ (d), $4\,\mu m$ (h), and $6\,\mu m$ (l). Amplitudes of interference fringes A_{intef} are indicated by dashed lines. $P_{ex} = 1.9\mu$W.

Figure 3 presents emission images I_1 for arm 1 open, emission images I_2 for arm 2 open, and interference images I_{12} for both arms open for different shifts δx. Figure 4 presents cross-sections of interference images I_{12} and $I_{\rm interf} = (I_{12} - I_1 - I_2)/(2\sqrt{I_1 I_2}\,)$ for different δx and temperatures.

Transition temperature.

In this section, we estimate the temperature of Bose-Einstein condensation (BEC) of excitons in the trap and compare it with the measured condensation temperature. For a rough estimate, we use the formula for BEC in a system of ideal noninteracting bosons in a parabolic 2D trap [3–5]: $T_c = \frac{\sqrt{6}}{\pi}\hbar\omega_{2D}\sqrt{N/g}$, where $\omega_{2D} = (\omega_x\omega_y)^{1/2}$,

ω_x and ω_y are the trap oscillator frequencies, g is the spin degeneracy, and N is the number of particles in the trap. A parabolic fit to the trap profile (Fig. 1c,d in the main text) $E(x, y) = \frac{m}{2}(\omega_x^2 x^2 + \omega_y^2 y^2)$ gives for $g = 4$ and exciton mass $m = 0.22 m_0$ [6]: $\omega_x \sim 4 \times 10^9$ s^{-1}, $\omega_y \sim 3 \times 10^{10}$ s^{-1}, and $T_c \sim 0.03\sqrt{N}$.

The exciton density n can be estimated from the energy shift. For the data in Fig. 5 at the lowest temperatures, the measured energy shift $\delta E \approx 1.3$ meV. Using the plate capacitor formula for the density estimate $\delta E = 4\pi e^2 n d/\varepsilon$ [7–9], where $d \approx 12$ nm is the separation between the electron and hole layers for our sample and ε is the background dielectric constant, gives $n \sim 10^{10}$ cm^{-2}. For the size of the exciton cloud in the trap ~ 10 μm^2 (Fig. 3 in the main text), a total exciton number in the trap $N \sim 10^3$. This gives $T_c \sim 1$ K.

The plate capacitor formula underestimates the density [10, 11]. Using the correction for the relation between δE and n estimated in [12], we obtain from the energy shift $N \sim 3 \times 10^3$ [13] and $T_c \sim 2$ K. These rough estimates of the temperature of exciton BEC in the trap are close to the measured transition temperature ~ 2 K (Fig. 5c in the main text).

[1] Hammack, A.T.; Gippius, N.A.; Sen Yang; Andreev, G.O.; Butov, L.V.; Hanson, M.; Gossard, A.C. Excitons in electrostatic traps. *J. Appl. Phys.* **2006**, 99, 066104

[2] Milonni, P.W.; Eberly, J.H. *Lasers* (Wiley, New York, 1988).

[3] Ketterle, W.; van Druten, N.J. Bose-Einstein condensation of a finite number of particles trapped in one or three dimensions. *Phys. Rev. A* **1996**, 54, 656

[4] Mullin, W.J.; Bose-Einstein Condensation in a Harmonic Potential. *J. Low Temp. Phys.* **1997**, 106, 615

[5] Dalfovo, F; Giorgini, S.; Pitaevskii, L.P.; Stringari, S. Theory of Bose-Einstein condensation in trapped gases. *Rev. Mod. Phys.* **1999**, 71, 463

[6] Butov, L.V.; Mintsev, A.V.; Lozovik, Yu.E.; Campman, K.L.; Gossard. A.C. From spatially indirect excitons to momentum-space indirect excitons by an in-plane magnetic field. *Phys. Rev. B* **2000**, 62, 1548

[7] Yoshioka, D.; MacDonald, A.H. Double Quantum Well Electron-Hole Systems in Strong Magnetic Fields. *J. Phys. Soc. Jpn.* **1990** 59, 4211

[8] Zhu, X; Littlewood, P.B.; Hybertsen, M.; Rice, T.M. Exciton Condensate in Semiconductor Quantum Well Structures. *Phys. Rev. Lett.* **1995** 74, 1633

[9] Ivanov, A.L. Quantum diffusion of dipole-oriented indirect excitons in coupled quantum wells. *Europhys. Lett.* **2002** 59, 586

[10] Schindler, C.; Zimmermann. R. Analysis of the exciton-exciton interaction in semiconductor quantum wells. *Phys. Rev. B* **2008** 78, 045313

[11] Ivanov. A.L.; Muljarov. E.A.; Mouchliadis. L.; Zimmermann. R. Comment on Photoluminescence Ring Formation in Coupled Quantum Wells: Excitonic Versus Ambipolar Diffusion. *Phys. Rev. Lett.* **2010** 104, 179701

[12] Remeika, M.; Graves, J.C.; Hammack, A.T.; Meyertholen, A.D.; Fogler, M.M.; Butov, L.V.; Hanson, M.; Gossard, A.C. Localization-delocalization transition of indirect excitons in lateral electrostatic lattices. *Phys. Rev. Lett.* **2009**, 102, 186803

[13] Note that the exciton density can be also roughly estimated from the light absorption: $n \sim \frac{P_{ex}}{E_{ex} A_{ex}} \alpha\tau$, where P_{ex} is the power of the excitation laser, E_{ex} is the photon energy of the excitation laser, A_{ex} is the excitation spot area, α is the fraction of photons emitted by the excitation laser that is transformed to indirect excitons due to the light absorption and carrier relaxation, and τ is the lifetime of indirect excitons. The uncertainty in the value of α makes such estimate rough. For $\alpha \sim 10^{-2}$, $P_{ex} \sim 2$ μW, $E_{ex} \sim 2$ eV, $A_{ex} \sim 10$ μm^2, and $\tau \sim 50$ ns, the estimate from the light absorption gives $n \sim 3 \times 10^{10}$ cm^{-2} and $N \sim 3 \times 10^3$.